

## Article

# Using Drones to Assess Volitional Swimming Kinematics of Manta Ray Behaviors in the Wild

Vicky Fong <sup>1,\*</sup> , Sarah L. Hoffmann <sup>2</sup> and Jessica H. Pate <sup>1</sup><sup>1</sup> Marine Megafauna Foundation, West Palm Beach, FL 33411, USA; jessica.pate@marinemegafauna.org<sup>2</sup> Merck Animal Health, Boise, ID 83702, USA; sarah.hoffmann@merck.com

\* Correspondence: vicky.fong@marinemegafauna.org

**Abstract:** Drones have become increasingly popular tools to study marine megafauna but are underutilized in batoid research. We used drones to collect video data of manta ray (*Mobula cf. birostris*) swimming and assessed behavior-specific kinematics in Kinovea, a semi-automated point-tracking software. We describe a ‘resting’ behavior of mantas making use of strong currents in man-made inlets in addition to known ‘traveling’ and ‘feeding’ behaviors. No significant differences were found between the swimming speed of traveling and feeding behaviors, although feeding mantas had a significantly higher wingbeat frequency than traveling mantas. Resting mantas swam at a significantly slower speed and wingbeat frequency, suggesting that they were continuously swimming with the minimum effort required to maintain position and buoyancy. Swimming speed and wingbeat frequency of traveling and feeding behaviors overlapped, which could point to other factors such as prey availability and a transitional behavior, influencing how manta rays swim. These baseline swimming kinematic data have valuable applications to other emerging technologies in manta ray research.

**Keywords:** manta ray; swimming; kinematics; behavior; drones

**Citation:** Fong, V.; Hoffmann, S.L.; Pate, J.H. Using Drones to Assess Volitional Swimming Kinematics of Manta Ray Behaviors in the Wild. *Drones* **2022**, *6*, 111. <https://doi.org/10.3390/drones6050111>

Academic Editors: Margarita Mulero-Pazmany and Barbara Bollard

Received: 2 April 2022

Accepted: 23 April 2022

Published: 28 April 2022

**Publisher’s Note:** MDPI stays neutral with regard to jurisdictional claims in published maps and institutional affiliations.



**Copyright:** © 2022 by the authors. Licensee MDPI, Basel, Switzerland. This article is an open access article distributed under the terms and conditions of the Creative Commons Attribution (CC BY) license (<https://creativecommons.org/licenses/by/4.0/>).

## 1. Introduction

Unmanned aerial vehicles (UAVs, commonly drones) have become increasingly popular tools to study animal behavior and habitat use in marine environments. Marine megafauna have traditionally been surveyed from the air in small planes and helicopters, but flights can be expensive and not readily available [1]. Since fine-scale behavior is difficult to observe from high altitudes, drones have shown potential to outperform traditional aerial surveys with manned aircrafts [1]. Thus, drones offer scientists an easily accessible, relatively inexpensive, and non-obtrusive solution to observe animals in their natural habitat, while simultaneously collecting video, photo, and geolocation data [2].

A broad range of marine megafauna has been studied using drones, including sea turtles [3–7], cetaceans [8–11] and elasmobranchs (sharks and rays) [12,13], and multiple species have also been surveyed simultaneously [14–22]. Despite their popularity in elasmobranch research, a recent review highlighted the underutilization of drone technology in batoid (ray) research compared to sharks [13]. Drone observations are generally restricted to animals that occupy shallow habitats with clear water, thus making it difficult to detect many batoid species that either live benthic lifestyles in murky waters or in deep habitats [13].

Manta rays (*Mobula* spp.) are ideal subjects for drone observations, as they tend to spend time in shallow, nearshore waters or at the surface to feed. Mantas are large, planktivorous elasmobranchs that are distributed globally in tropical and subtropical waters [23]. Living completely pelagic lifestyles, manta rays are negatively buoyant obligate ram ventilators that must keep swimming to stay afloat and move water over their gills [24]. Unlike their benthic relatives, mantas swim primarily by dorsoventral oscillation (flapping) of the

pectoral fins reminiscent of some aerial flyers, which generates lift with high propulsive efficiency [25]. These efficient swimmers are capable of long-distance migrations [26–30], but more frequently demonstrate high site fidelity and residency [31–43]. The two known manta species (*Mobula birostris* and *Mobula alfredi*) have been listed as endangered and vulnerable, respectively, on the IUCN Red List, predominantly due to targeted fishing and bycatch [44,45]. Slow life-history traits of manta rays, including low fecundity, long gestation period, and late age of maturity, make them more vulnerable to overexploitation [46–48]. Anthropogenic threats continue to affect declining global populations, and large knowledge gaps still exist for manta rays [49,50].

Drones have previously been used in other populations to study collective movement of manta rays as well as to identify individuals and measure body size [51–53], but not to quantify kinematics. Determining how kinematics vary among behaviors is crucial to understanding how manta rays utilize their habitat. Behavior-correlated swimming speeds have been extrapolated from manta ray satellite telemetry data [26,54], which provide insightful information on large-scale movement patterns, but lack fine-scale data necessary for kinematic analyses, as behaviors were inferred and not directly observed. Previously, researchers have relied on estimations of swimming speeds in the field to calculate prey density threshold of mantas, but empirical measurements of swimming speed would improve inference for future studies on feeding ecology, migration, and energetics [55,56]. Manta ray swimming kinematics were previously assessed in aquaria [25] and in the wild [57], but swimming in captivity is spatially restricted and in situ data were limited to a fixed camera at a single cleaning station. The use of drones, however, provides a discreet and mobile alternative to resource-intensive underwater imagery for studying wild, volitional swimming of manta rays.

This study presents a novel application of drone-based imagery to quantify the swimming kinematics of manta rays across a range of behaviors. ‘Traveling’ (also known as ‘directed swimming’, ‘cruising’ or ‘transiting’) and ‘feeding’ behaviors were previously recorded for this population [42], and here we additionally describe ‘resting’ behavior of manta rays utilizing strong currents for ram ventilation inside man-made inlets. We predict that (1) there is a positive relationship between swimming speed and wingbeat frequency; (2) feeding mantas swim slower to optimize filter feeding in dense plankton patches, (3) traveling mantas swim faster for more efficient transits, and (4) resting mantas have a slower wingbeat frequency to conserve energy. Better understanding of behavior-correlated swimming kinematics of manta rays can shed light on their habitat use and possibly inform conservation measures for their protection.

## 2. Materials and Methods

### 2.1. Study Site

A manta ray nursery habitat has recently been described along the coast of southeastern Florida, United States of America [42]. Despite being listed as a threatened species on the US Endangered Species Act in 2018, insufficient data exist on manta populations in the US to designate critical habitat [42]. Genetic studies suggest that Florida mantas are a putative third species of manta ray (*M. cf. birostris*), but it has yet to be formally described [58,59]. Utilization of drones have drastically improved the ability to locate and monitor manta rays in this population. Drones were launched during boat and shore-based surveys from September 2020 to December 2021 to locate manta rays along a north–south transect between St. Lucie Inlet (27°09′47″ N, 80°09′27″ W) and Boynton Beach Inlet (26°32′44″ N, 80°02′31″ W), Florida, USA [42].

### 2.2. Data Collection

We used a drone (DJI Mavic Pro 2; Shenzhen Dajiang Baiwang Technology Co., Ltd., Shenzhen, China) mounted 1 in CMOS, 4K video camera with a polarizing filter to collect videos of manta rays swimming. Drone flights were conducted approximately 200 m from the shore at altitudes of approximately 100 m to maximize our search area. When a manta

ray was located, we lowered the drone to an altitude of less than 15 m while hovering such that all parts of the animal's body were clearly visible in the field of view. The camera was positioned orthogonal to the water surface to minimize distortion and ensure all videos were comparable. Hovering continued until the animal entirely exited the field of view. All videos were recorded at a resolution of  $3840 \times 2160$  pixels and 29.97 frames per second. Videos were subsequently clipped into 5 to 20 s segments (mean = 10.3 s) for kinematic analyses.

For each clip, manta ray behavior was classified as 'traveling', 'feeding' or 'resting' (Table 1); 23, 20 and 7 clips were collected for each behavior, respectively. Different feeding strategies, including surface feeding, have previously been described [24], and although our mantas were observed feeding near the surface, their bodies never broke the surface of the water. Behavior was classified based on the entire encounter with the manta ray and not solely on the clip used for kinematic analysis [39,42].

**Table 1.** Descriptions of behaviors exhibited by manta rays.

Behavior	Description
Traveling	Cephalic fins rolled, mouth closed (if visible), maintaining directional heading while swimming
Feeding	Cephalic fins unrolled with tips often touching, mouth open (if visible), changing directions while swimming
Resting	Facing into strong current to maintain stationary position, located inside inlet

When conditions were suitable for a snorkeler to enter the water, visual identification photographs of the ventral spot pattern were collected to identify the manta ray individual [60]. Manta rays were measured opportunistically using underwater paired-laser photogrammetry [61], where a GoPro camera centered between parallel laser pointers 60 cm apart captured images orthogonal to the ray's body, which were then processed in Image J (v.1.53) to measure disc length based on the known distance between laser points [61].

### 2.3. Kinematic Analyses

Clips were digitized by one author (V.F.) using Kinovea (v.0.9.5) [62], a free, open-source video annotation tool with point-tracking capability. Three anatomical landmarks—one on each tip of the pectoral fins (to calculate wingbeat frequency) and the base of the tail (to measure swimming speed)—were tracked. Once the anatomical landmark (Figure 1) was identified in frame 1, tracking was automated by the software, allowing for more efficient video analysis compared to using manual point-tracking software. To ensure the selected anatomical landmark was being tracked accurately, any points that deviated from the actual path of movement were corrected. Relative time and  $x, y$  cartesian coordinates of completed tracks were exported as an XML file for further analyses.

For each clip, the pectoral fin tracks were visualized (Microsoft Excel v.16.56) to determine start and end points (the peak of an oscillation) of each wingbeat cycle, defined as the time between two peaks. Each clip consisted of at least two wingbeats (range = 2–6, mean = 3.5). The corresponding timestamps were identified to calculate the period ( $T$ ; s) of each wingbeat cycle. The average duration of wingbeat period ( $T_{av}$ ; s) was calculated for each clip, and average wingbeat frequency ( $f$ ; hz) was calculated as:

$$f = 1/T_{av}. \quad (1)$$

Kinematic analyses were standardized by body length (BL), measured as the midline distance (pixels) from the mouth to the base of the tail, to compare across individuals and clips (Figure 1). The  $x, y$  coordinates of the tail base between video frames were used to calculate instantaneous speed ( $U_i$ ;  $BL \cdot s^{-1}$ ) as:

$$U_i = \sqrt{(X(n+1) - X_n)^2 + (Y(n+1) - Y_n)^2} / t \quad (2)$$

where the distance (BL) between  $X_n Y_n$  (tail base position in frame  $n$ ) and  $X_{n+1} Y_{n+1}$  (tail base position in the subsequent frame) is divided by  $t$  (time between frames). Overall clip speed ( $U_{av}$ ;  $BL \cdot s^{-1}$ ) was calculated as the average of  $U_i$  for the duration of the clip.

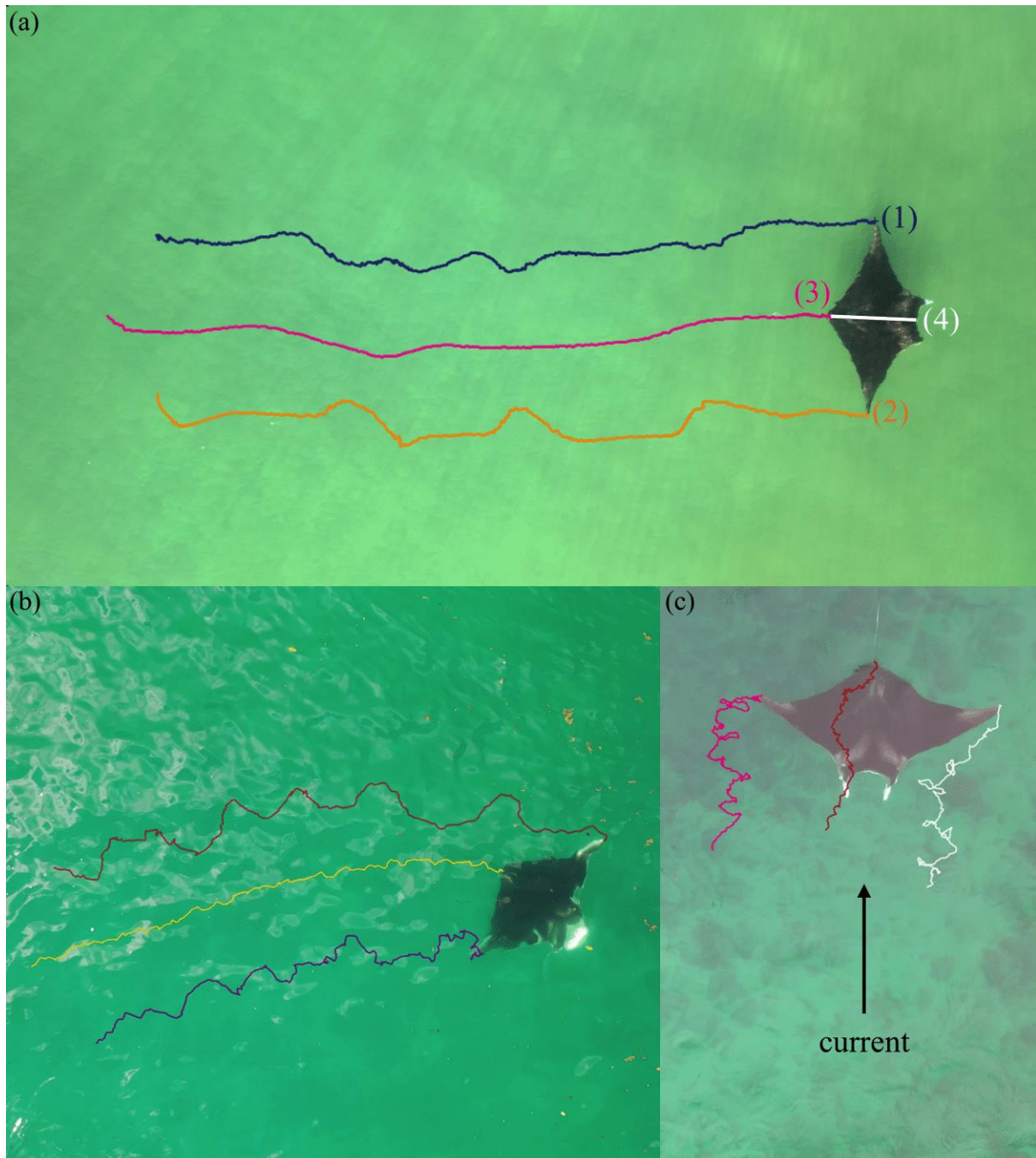


**Figure 1.** Screen capture of manta ray swimming clips in Kinovea after point-tracking was completed. Behaviors displayed are (a) traveling, (b) feeding, and (c) resting. Paths of three anatomical landmarks are marked as (1) tip of left pectoral fin, (2) tip of right pectoral fin, and (3) base of tail. The white line (4) marks body length that is measured as midline distance from mouth to base of tail. Full videos can be found in the Supplementary Materials.

In another analysis, body length (m) was measured for six individuals using in-water laser photogrammetry. Thirteen clips that included those individuals were additionally standardized by BL (m) and fine-scale swimming speeds ( $m \cdot s^{-1}$ ) were calculated (Equation (2)).

To see whether fine-scale swimming speeds could reasonably be extrapolated to large-scale movements, large-scale swimming speeds ( $\text{m}\cdot\text{s}^{-1}$ ) were also calculated for individuals ( $n = 6$ ) that were seen multiple times in consecutive days on boat surveys and if identified to be traveling in all encounters. Based on the locations where manta individuals were sighted and directional heading, a minimum swimming speed was estimated using straight-line distance (over water) and time elapsed between encounters.

#### 2.4. Statistical Analysis

The relationship between speed ( $U_{av}$ ) and wingbeat frequency ( $f$ ) was visualized for each behavior and analyzed for significance using a one-way ANOVA with Tukey HSD post hoc analyses (RStudio v.1.3.1093). When ANOVA assumptions were violated (Levene test for equal variances, Shapiro–Wilk test for normality), a non-parametric alternative (Kruskal–Wallis rank sum test) was used. All means were reported  $\pm$  standard error of the mean. A two-tailed  $t$  test was used to determine significant differences between fine and large-scale swimming speeds ( $\text{m}\cdot\text{s}^{-1}$ ).

### 3. Results

Fifty manta ray swimming clips were analyzed where behaviors were clearly defined as traveling ( $n = 23$ ), feeding ( $n = 20$ ) or resting ( $n = 7$ ). The smaller sample size for resting was due to a lesser likelihood of encountering the behavior. All manta rays observed were juveniles based on underwater observation of immature claspers (males) or size estimations (females) [42]. Kinematic analyses revealed that speed is positively correlated to wingbeat frequency across all behaviors (Figure 2; Traveling  $R = 0.349$ ; Feeding  $R = 0.207$ ; Resting  $R = 0.081$ ). While feeding and traveling behaviors had overlapping velocities and wingbeat frequencies, resting behavior was isolated at the lesser ranges of both speed and wingbeat frequency (Figure 2).

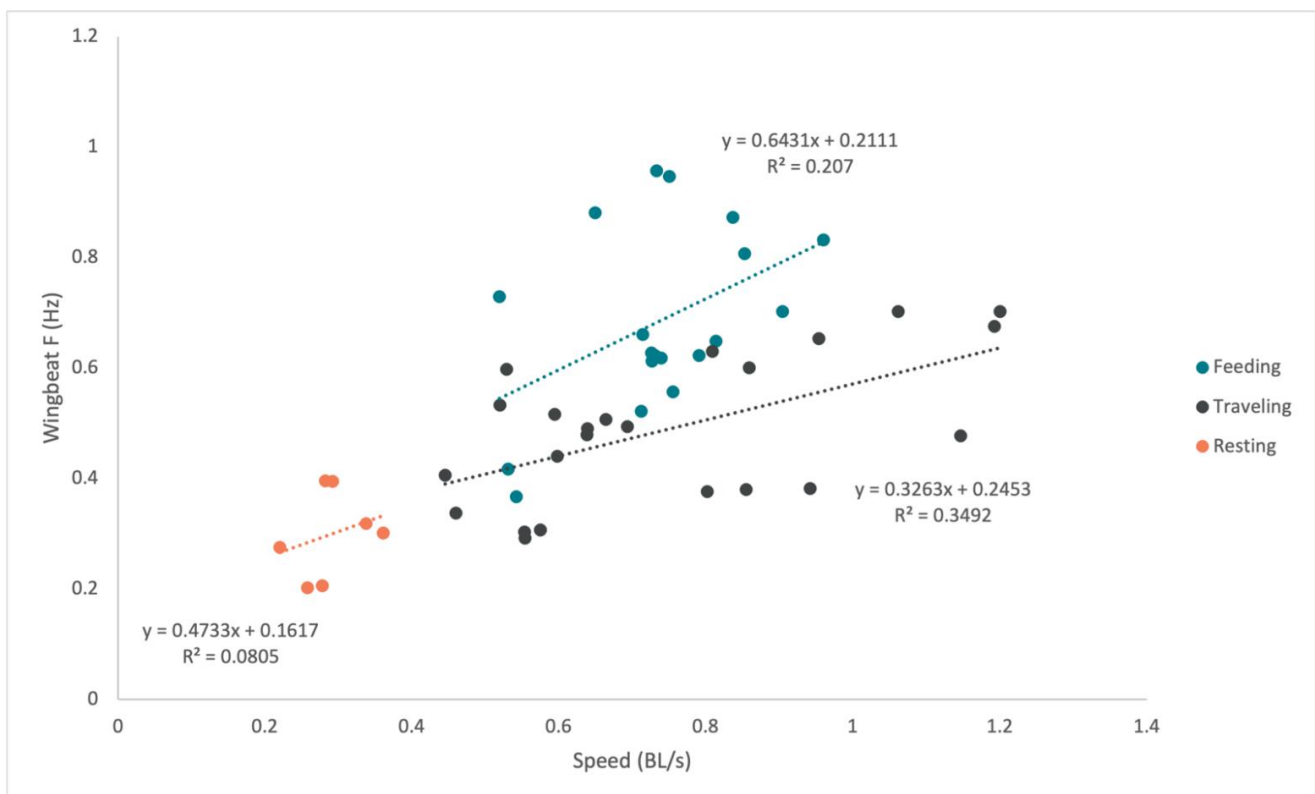


**Figure 2.** Relationship between speed and wingbeat frequency in manta ray swimming. Manta ray behaviors are denoted by color.

Traveling mantas had the fastest mean speed ( $0.752 \pm 0.049 \text{ BL}\cdot\text{s}^{-1}$ ), followed by feeding mantas ( $0.727 \pm 0.027 \text{ BL}\cdot\text{s}^{-1}$ ), and resting mantas ( $0.290 \pm 0.018 \text{ BL}\cdot\text{s}^{-1}$ ) (Figure 3). Kruskal–Wallis rank sum test indicated a significant difference in velocities between behaviors [ $H(2) = 17.734, p = 0.0001$ ]. Post hoc tests showed significant differences between resting and feeding ( $p = 0.000004$ ), and resting and traveling ( $p = 0.000001$ ), but not between traveling and feeding ( $p = 0.9$ ).

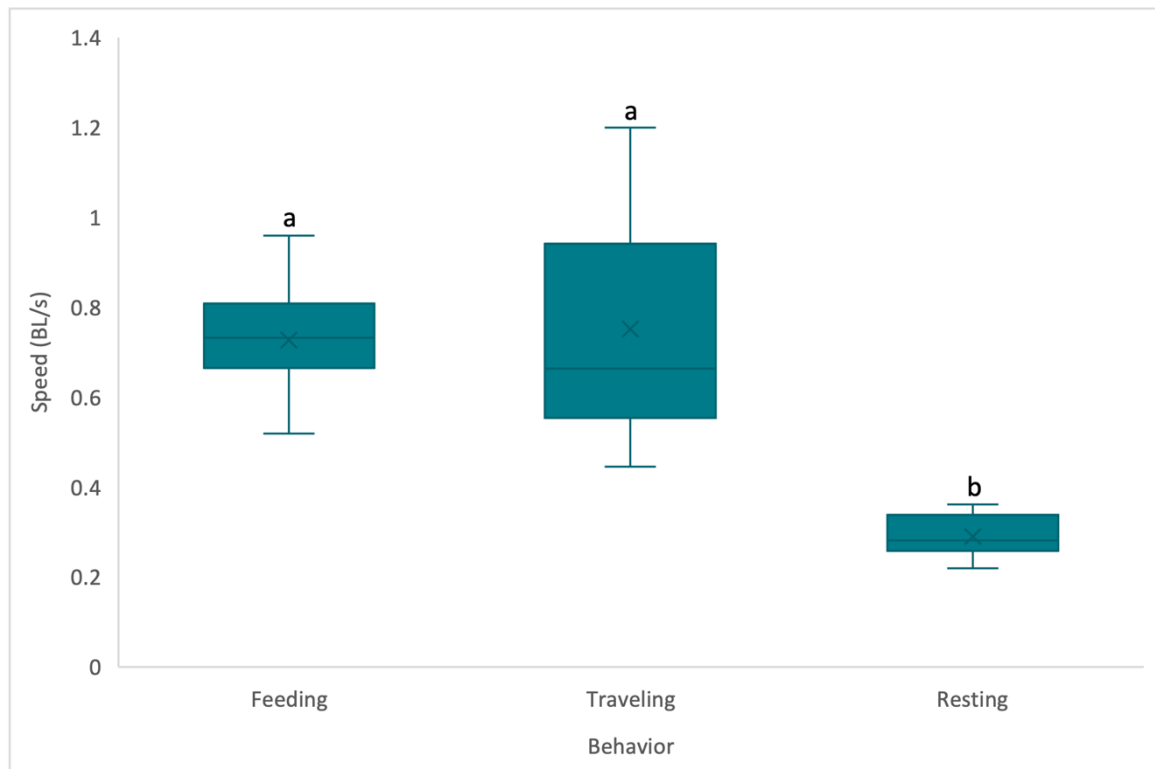


**Figure 3.** Speed of manta ray swimming based on behavior. Boxes represent the exclusive medians (middle line) and interquartile range, x marks the means, and whiskers represent the minimum and maximum values. Letters above box plots denote significant differences.

Feeding mantas had the greatest wingbeat frequency ( $0.667 \pm 0.040 \text{ Hz}$ ), followed by traveling mantas ( $0.491 \pm 0.027 \text{ Hz}$ ) and resting mantas ( $0.340 \pm 0.047 \text{ Hz}$ ) (Figure 4). One-way ANOVA showed significant differences [ $F(2, 47) = 18.01, p = 0.000002$ ] between wingbeat frequency and behavior. Post hoc tests confirmed that differences between all behavior pairs were statistically significant: resting and feeding ( $p = 0.000002$ ), traveling and feeding ( $p = 0.0008$ ), traveling and resting ( $p = 0.01$ ).

Body lengths of manta ray individuals were measured using paired-laser photogrammetry for six individuals (range = 0.94–1.24 m, mean = 1.11 m) over thirteen encounters, and fine-scale swimming speeds ( $\text{m}\cdot\text{s}^{-1}$ ) were calculated: four feeding mantas swam at  $0.746 \pm 0.043 \text{ m}\cdot\text{s}^{-1}$ , and nine traveling mantas swam at  $0.718 \pm 0.071 \text{ m}\cdot\text{s}^{-1}$ . Six large-scale swimming speeds were calculated based on approximate distance traveled between encounters averaged  $0.687 \pm 0.107 \text{ m}\cdot\text{s}^{-1}$ , ranging between 0.303 and  $1.0 \text{ m}\cdot\text{s}^{-1}$ . Distance traveled ranged from 2340 to 60,600 m, and time elapsed between encounters ranged from 2340 to 91,800 s. A two-tailed  $t$  test found no significant differences between fine and large-scale swimming speeds of traveling mantas [ $t(13) = 0.2, p = 0.8$ ].

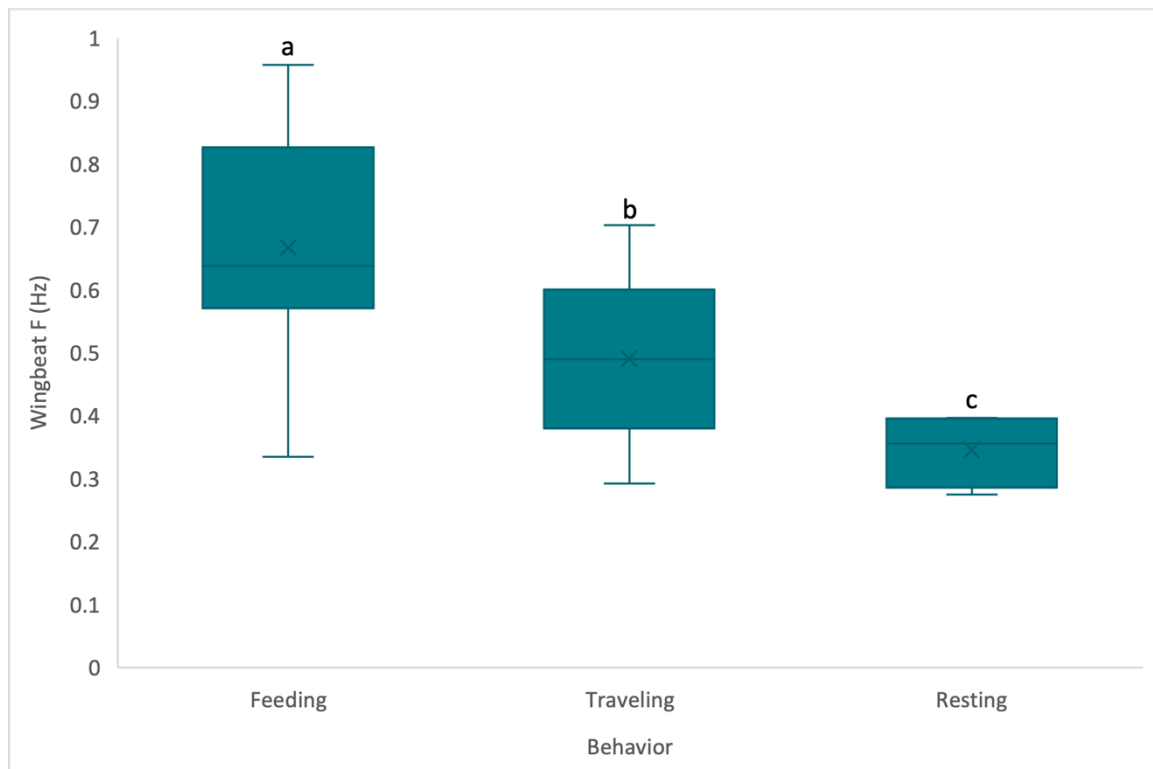


**Figure 4.** Wingbeat frequency of manta ray swimming based on behavior. Boxes represent the exclusive medians (middle line) and interquartile range, x marks the means, and whiskers represent the minimum and maximum values. Letters above box plots denote significant differences.

#### 4. Discussion

Our study employed a method of aerial drone analyses to evaluate fine-scale kinematics of wild, volitional manta ray swimming. We found an overall positive correlation between swimming speed and wingbeat frequency across all behaviors observed (Figure 2). This supports previous research showing that the frequency of oscillation in manta ray pectoral fins increased directly with swimming speed [57]. The degree to which swimming speed and wingbeat frequency were correlated, however, varied between behaviors.

We observed the greatest mean swimming speed and the most variation in traveling mantas (Figure 3). The goal of traveling is likely to cover as much distance as possible or to reach a destination with greatest efficiency. As such, animals may optimize their hydrodynamic efficiency, as seen in mantas rolling up cephalic fins to reduce drag while swimming and conserve energy while traveling [63]. Since no significant differences were found between fine-scale ( $0.718 \text{ m}\cdot\text{s}^{-1}$ ) and large-scale swimming speeds ( $0.687 \text{ m}\cdot\text{s}^{-1}$ ), we propose that fine-scale swimming speeds can be reasonably extrapolated to larger-scale movements, but are slower than previously reported swimming speeds of traveling mantas ( $0.97 \text{ m}\cdot\text{s}^{-1}$ ) calculated from satellite telemetry data [26]. Wingbeat frequencies of traveling mantas were significantly slower and presented less variation than feeding individuals (Figure 4). This could indicate that mantas perform less labored swimming while traveling, as there is less incentive to expend more energy, thus relying on the gliding phase between each wingbeat [57]. Similarly, aquatic birds have been shown to expend less energy on commuting flights than foraging dives, suggesting that in situations of low prey density, animals can optimize efficiency by making long commutes to areas where foraging efficiency is high [64].

Previous satellite telemetry studies showed that feeding mantas swam significantly slower ( $0.11 \text{ m}\cdot\text{s}^{-1}$  [26],  $0.33 \text{ m}\cdot\text{s}^{-1}$  [54]) than traveling mantas ( $0.97 \text{ m}\cdot\text{s}^{-1}$  [26]), but the data collected were not fine scale, and behavior was inferred rather than observed. In this study, feeding mantas had a marginally slower, yet not significantly different, mean

swimming speed and less variation than traveling mantas (Figure 3). Differences in prey availability may result in slower swimming, as manta rays are thought to accelerate when feeding in low-density plankton patches to maximize prey encounters and decelerate in high-density plankton areas to conserve energy [65]. This relationship should be further investigated by deploying zooplankton tows to collect food samples simultaneously with drone footage of feeding mantas, to directly compare prey size, type, and abundance with swimming kinematics.

Despite slower swimming speeds, feeding mantas had the greatest mean wingbeat frequency across behaviors and showed the greatest variation in wingbeat frequency (Figure 4). The high energetic cost of feeding needs to be compensated by an even higher energy intake [56], thus mantas will regularly change their directional heading to move to wherever food is available, requiring more frequent and sporadic wingbeat cycles. To perform turning maneuvers, mantas either execute powered turns through asymmetrical propulsive motions of pectoral fins, or unpowered turns through banking (a rolling maneuver) that is achieved by lift-based centripetal force of the pectoral fins [57], both of which could cause an increase in wingbeat frequency. These maneuvers require asynchronous fin movements that could potentially cause a destabilizing force, making the manta more agile for rapid maneuvers [66]. While we cannot distinguish between powered and unpowered turns without lateral views of swimming, both maneuvers to some extent rely on unsteady motions of pectoral fins, and subsequently greater wingbeat frequency, to change orientation and direction [57].

We predicted greater differentiation in kinematics between traveling and feeding behaviors, but it is evident that swimming speed and wingbeat frequency alone are insufficient to predict behavior (Figure 2). This could point to other factors, such as current direction and strength, tides, prey availability, human interaction, and boating and fishing interactions, that could influence the way a manta ray swims. It could also be evidence for mantas exhibiting a fourth cryptic behavior that was not classified in this study. Papastamatiou et al. (2012) actively tracked manta rays in small lagoons at Palmyra Atoll, where mantas showed 'area-restricted searching' behavior to move between or locate high-density plankton patches, which allowed them to remain in a small area to maximize resource acquisition [67]. Although no kinematic data were available from the acoustic tracking study, 'area-restricted searching' individuals swam with more tortuous movements and performed more turns in comparison to straighter transiting movements [67], suggesting that swimming speed and wingbeat frequency could differ from those of traveling and feeding behaviors. While study results from a confined spatial scale (i.e., a small atoll lagoon) are difficult to extrapolate to movements at a larger scale, such as our mantas swimming along a coastline, it hints at a potential transitional behavior between traveling and feeding and warrants further investigation into how prey availability could impact behavior-correlated kinematics and movement patterns.

Resting mantas had a significantly slower mean swimming speed and wingbeat frequency than other behaviors (Figures 3 and 4). In this instance, we suspect that manta rays likely utilize a strong current for ventilation to conserve energy. Further, we propose that the limited variation observed in these data may suggest that resting mantas are continuously swimming with the minimum effort required to maintain position and remain buoyant. This behavior has also been observed in narrow channels with strong currents in Indonesia [68], but it has yet to be quantified or formally described. A recent study discussed how another negatively buoyant obligate-swimmer species, grey reef shark (*Carcharhinus amblyrhynchos*), uses current updrafts to reduce energy expenditure [69]. Compared to the current ( $\sim 0.5 \text{ m}\cdot\text{s}^{-1}$ ) faced by the grey reef sharks [69], the manta rays in this study may have been utilizing a much stronger current with a mean speed of  $1.086 \text{ m}\cdot\text{s}^{-1}$  [70].

Manta rays resting inside man-made inlets is a concerning phenomenon due to intense boat traffic and fishing as a popular activity in these areas. Almost half of the juvenile manta ray individuals in south Florida have scars or injuries, many from anthropogenic

impacts [42]. Future kinematic studies should focus on the impacts of manta rays living in high-density human presence, including potential negative impacts of boat and fishing injuries on swimming performance. Previous studies have reported qualitative behavioral responses of manta rays toward in-water tourism, including changes in swimming speed [71,72], thus the effects of tourism should be further investigated by comparing swimming kinematics before, during, and after interactions with snorkelers. Since this study measured the kinematics of swimming in a juvenile population of manta rays, caution should be exercised when applying these data to adult populations. Future work should focus on how kinematics can change with ontogeny, as swimming speeds are known to vary through growth in some animals [73]. Quantifying other behaviors, such as courtship and mating, would also be valuable, as swimming speed has been qualitatively described to vary across different stages of courtship-trains in manta rays [74,75]. Moreover, our methodology can be used to compare the swimming kinematics of the other species and populations of manta rays, as well as other batoids.

Baseline swimming kinematics of manta rays have valuable applications to other research topics and emerging technologies. We presented behavior-correlated kinematics that could be used to validate data from accelerometers and satellite telemetry by using machine learning to rapidly identify and model behaviors from animal tracks [76–78]. Other applications of fine-scale kinematics have included biomechanical studies to better understand the filtration mechanism of gill plates in manta rays [79]. Results from our study can also be applied to areas such as feeding ecology to improve the reliability of prey density threshold measurements, and lay groundwork for improved bioenergetic modeling across manta ray behaviors as swimming speed is an essential kinematic parameter in these models [80]. Additionally, we described resting behavior that is especially difficult to observe without drones, as divers cannot enter the water due to the proximity to fast-moving vessels. Fundamentally, we present a novel, minimally invasive technique to quantify swimming kinematics and behavior and the first ever empirically measured volitional swimming kinematics of manta rays in the wild. Better understanding of manta ray swimming performance not only sheds light on their habitat use but has the potential to improve conservation management practices of these increasingly vulnerable species.

**Supplementary Materials:** The following supporting information can be downloaded at: <https://www.mdpi.com/article/10.3390/drones6050111/s1>, Video S1: example of traveling manta ray; Video S2: example of feeding manta ray; Video S3: example of resting manta ray.

**Author Contributions:** Conceptualization, J.H.P.; Methodology, J.H.P. and S.L.H.; Software, V.F.; Validation, V.F., J.H.P. and S.L.H.; Formal Analysis, V.F.; Investigation, J.H.P. and V.F.; Resources, J.H.P.; Data Curation, V.F.; Writing—Original Draft Preparation, V.F.; Writing—Review and Editing, J.H.P. and S.L.H.; Visualization, V.F.; Supervision, J.H.P.; Project Administration, J.H.P.; Funding Acquisition, J.H.P. All authors have read and agreed to the published version of the manuscript.

**Funding:** Boat surveys were funded by a Disney Conservation Fund grant awarded to J.H.P.

**Data Availability Statement:** The data presented in this study are available upon request from the corresponding author. The data are not publicly available due to large file sizes of multimedia.

**Acknowledgments:** The authors would like to thank the many volunteers of the Florida Manta Project who made this work possible. We would also like to thank three anonymous reviewers for their comments on the manuscript.

**Conflicts of Interest:** The authors declare no conflict of interest.

## References

1. Colefax, A.P.; Butcher, P.A.; Kelaher, B.P. The Potential for Unmanned Aerial Vehicles (UAVs) to Conduct Marine Fauna Surveys in Place of Manned Aircraft. *ICES J. Mar. Sci.* **2018**, *75*, 1–8. [CrossRef]
2. Porter, M.E.; Ruddy, B.T.; Kajiura, S.M. Volitional Swimming Kinematics of Blacktip Sharks, *Carcharhinus limbatus*, in the Wild. *Drones* **2020**, *4*, 78. [CrossRef]

3. Tapilatu, R.F.; Bonka, A.N.; Iwanggin, W.G.; Wona, H.; Woisiri, S.; Sembor, E.; Rumbiak, R.; Ampnir, T.; Bawole, R.; Wibbels, T. Utilizing Drone Technology to Assess Leatherback Sea Turtle (*Dermochelys coriacea*) Hatchling Fitness. In Proceedings of the Connections through Shallow Seas, Papua Barat, Indonesia, 6 July 2017.
4. Tapilatu, R.F.; Bonka, A.N.; Iwanggin, W.G.; Wona, H.; Ampnir, T.; Rumbiak, R.; Bawole, R.; Wibbels, T. Unmanned Aerial Vehicle (UAV) Use as a Tool to Assess Crawling and Swimming Speeds in Hatchling Sea Turtles. *Herpetol. Rev.* **2019**, *50*, 722–726.
5. Gray, P.C.; Fleishman, A.B.; Klein, D.J.; McKown, M.W.; Bézy, V.S.; Lohmann, K.J.; Johnston, D.W. A Convolutional Neural Network for Detecting Sea Turtles in Drone Imagery. *Methods Ecol. Evol.* **2019**, *10*, 345–355. [[CrossRef](#)]
6. Schofield, G.; Esteban, N.; Katselidis, K.A.; Hays, G.C. Drones for Research on Sea Turtles and Other Marine Vertebrates—A Review. *Biol. Conserv.* **2019**, *238*, 108214. [[CrossRef](#)]
7. Odzer, M.N.; Brooks, A.M.L.; Heithaus, M.R.; Whitman, E.R. Effects of Environmental Factors on the Detection of Subsurface Green Turtles in Aerial Drone Surveys. *Wildl. Res.* **2022**, *49*, 79–88. [[CrossRef](#)]
8. Koski, W.R.; Gamage, G.; Davis, A.R.; Mathews, T.; LeBlanc, B.; Ferguson, S.H. Evaluation of UAS for Photographic Re-Identification of Bowhead Whales, *Balaena mysticetus*. *J. Unmanned Veh. Syst.* **2015**, *3*, 22–29. [[CrossRef](#)]
9. Durban, J.W.; Fearnbach, H.; Barrett-Lennard, L.G.; Perryman, W.L.; Leroi, D.J. Photogrammetry of Killer Whales Using a Small Hexacopter Launched at Sea. *J. Unmanned Veh. Syst.* **2015**, *3*, 131–135. [[CrossRef](#)]
10. Gough, W.T.; Segre, P.S.; Bierlich, K.C.; Cade, D.E.; Potvin, J.; Fish, F.E.; Dale, J.; di Clemente, J.; Friedlaender, A.S.; Johnston, D.W.; et al. Scaling of Swimming Performance in Baleen Whales. *J. Exp. Biol.* **2019**, *222*, jeb204172. [[CrossRef](#)] [[PubMed](#)]
11. Fettermann, T.; Fiori, L.; Gillman, L.; Stockin, K.A.; Bollard, B. Drone Surveys Are More Accurate Than Boat-Based Surveys of Bottlenose Dolphins (*Tursiops Truncatus*). *Drones* **2022**, *6*, 82. [[CrossRef](#)]
12. Butcher, P.A.; Colefax, A.P.; Gorkin, R.A., III; Kajiura, S.M.; López, N.A.; Mourier, J.; Purcell, C.R.; Skomal, G.B.; Tucker, J.P.; Walsh, A.J.; et al. The Drone Revolution of Shark Science: A Review. *Drones* **2021**, *5*, 8. [[CrossRef](#)]
13. Oleksyn, S.; Tosetto, L.; Raoult, V.; Joyce, K.E.; Williamson, J.E. Going Batty: The Challenges and Opportunities of Using Drones to Monitor the Behaviour and Habitat Use of Rays. *Drones* **2021**, *5*, 12. [[CrossRef](#)]
14. Kiszka, J.J.; Mourier, J.; Gastrich, K.; Heithaus, M.R. Using Unmanned Aerial Vehicles (UAVs) to Investigate Shark and Ray Densities in a Shallow Coral Lagoon. *Mar. Ecol. Prog. Ser.* **2016**, *560*, 237–242. [[CrossRef](#)]
15. Bevan, E.; Whiting, S.; Tucker, T.; Guinea, M.; Raith, A.; Douglas, R. Measuring Behavioral Responses of Sea Turtles, Saltwater Crocodiles, and Crested Terns to Drone Disturbance to Define Ethical Operating Thresholds. *PLoS ONE* **2018**, *13*, e0194460. [[CrossRef](#)] [[PubMed](#)]
16. Hensel, E.; Wenclawski, S.; Layman, C. Using a Small, Consumer Grade Drone to Identify and Count Marine Megafauna in Shallow Habitats. *Lat. Am. J. Aquat. Res.* **2018**, *46*, 1025–1033. [[CrossRef](#)]
17. Gallagher, A.J.; Papastamatiou, Y.P.; Barnett, A. Apex Predatory Sharks and Crocodiles Simultaneously Scavenge a Whale Carcass. *J. Ethol.* **2018**, *36*, 205–209. [[CrossRef](#)]
18. Colefax, A.P.; Butcher, P.A.; Pagendam, D.E.; Kelaher, B.P. Reliability of Marine Faunal Detections in Drone-Based Monitoring. *Ocean. Coast. Manag.* **2019**, *174*, 108–115. [[CrossRef](#)]
19. Kelaher, B.P.; Peddemors, V.M.; Hoade, B.; Colefax, A.P.; Butcher, P.A. Comparison of Sampling Precision for Nearshore Marine Wildlife Using Unmanned and Manned Aerial Surveys. *J. Unmanned Veh. Syst.* **2019**, *8*, 30–43. [[CrossRef](#)]
20. Frixione, M.G.; Gómez García Gauger, M.d.J.; Gauger, M.F.W. Drone Imaging of Elasmobranchs: Whale Sharks and Golden Cownose Rays Co-Occurrence in a Zooplankton Hot-Spot in Southwestern Sea of Cortez. *Food Webs* **2020**, *24*, e00155. [[CrossRef](#)]
21. Barreto, J.; Cajaíba, L.; Teixeira, J.B.; Nascimento, L.; Giacomo, A.; Barcelos, N.; Fettermann, T.; Martins, A. Drone-Monitoring: Improving the Detectability of Threatened Marine Megafauna. *Drones* **2021**, *5*, 14. [[CrossRef](#)]
22. Pirota, V.; Hocking, D.P.; Igglelen, J.; Harcourt, R. Drone Observations of Marine Life and Human–Wildlife Interactions off Sydney, Australia. *Drones* **2022**, *6*, 75. [[CrossRef](#)]
23. Marshall, A.D.; Compagno, L.J.V.; Bennett, M.B. Redescription of the Genus *Manta* with Resurrection of *Manta Alfredi* (Krefft, 1868) (Chondrichthyes; Myliobatoidei; Mobulidae). *Zootaxa* **2009**, *2301*, 1–28. [[CrossRef](#)]
24. Stevens, G.; Fernando, D.; Di Sciara, G.N. *Guide to the Manta and Devil Rays of the World*; Princeton University Press: Princeton, NJ, USA, 2018; ISBN 9780691183329.
25. Fish, F.E.; Schreiber, C.M.; Moored, K.W.; Liu, G.; Dong, H.; Bart-Smith, H. Hydrodynamic Performance of Aquatic Flapping: Efficiency of Underwater Flight in the Manta. *Aerospace* **2016**, *3*, 20. [[CrossRef](#)]
26. Jaine, F.R.A.; Rohner, C.A.; Weeks, S.J.; Couturier, L.I.E.; Bennett, M.B.; Townsend, K.A.; Richardson, A.J. Movements and Habitat Use of Reef Manta Rays off Eastern Australia: Offshore Excursions, Deep Diving and Eddy Affinity Revealed by Satellite Telemetry. *Mar. Ecol. Prog. Ser.* **2014**, *510*, 73–86. [[CrossRef](#)]
27. Germanov, E.S.; Marshall, A.D. Running the Gauntlet: Regional Movement Patterns of *Manta Alfredi* through a Complex of Parks and Fisheries. *PLoS ONE* **2014**, *9*, e110071.
28. Armstrong, A.O.; Armstrong, A.J.; Bennett, M.B.; Richardson, A.J.; Townsend, K.A.; Dudgeon, C.L. Photographic Identification and Citizen Science Combine to Reveal Long Distance Movements of Individual Reef Manta Rays *Mobula Alfredi* along Australia's East Coast. *Mar. Biodivers. Rec.* **2019**, *12*, 1–6. [[CrossRef](#)]
29. Harris, J.L.; McGregor, P.K.; Oates, Y.; Stevens, G.M.W. Gone with the Wind: Seasonal Distribution and Habitat Use by the Reef Manta Ray (*Mobula alfredi*) in the Maldives, Implications for Conservation. *Aquat. Conserv.* **2020**, *30*, 1649–1664. [[CrossRef](#)]

30. Armstrong, A.J.; Armstrong, A.O.; McGregor, F.; Richardson, A.J.; Bennett, M.B.; Townsend, K.A.; Hays, G.C.; van Keulen, M.; Smith, J.; Dudgeon, C.L. Satellite Tagging and Photographic Identification Reveal Connectivity Between Two UNESCO World Heritage Areas for Reef Manta Rays. *Front. Mar. Sci.* **2020**, *7*, 725. [[CrossRef](#)]
31. Dewar, H.; Mous, P.; Domeier, M.; Muljadi, A.; Pet, J.; Whitty, J. Movements and Site Fidelity of the Giant Manta Ray, *Manta birostris*, in the Komodo Marine Park, Indonesia. *Mar. Biol.* **2008**, *155*, 121–133. [[CrossRef](#)]
32. Couturier, L.I.E.; Jaine, F.R.A.; Townsend, K.A.; Weeks, S.J.; Richardson, A.J.; Bennett, M.B. Distribution, Site Affinity and Regional Movements of the Manta Ray, *Manta alfredi* (Kreffft, 1868), along the East Coast of Australia. *Mar. Freshw. Res.* **2011**, *62*, 628–637. [[CrossRef](#)]
33. Deakos, M.H.; Baker, J.D.; Bejder, L. Characteristics of a Manta Ray (*Manta alfredi*) population off Maui, Hawaii, and Implications for Management. *Mar. Ecol. Prog. Ser.* **2011**, *429*, 245–260. [[CrossRef](#)]
34. Marshall, A.D.; Dudgeon, C.L.; Bennett, M.B. Size and Structure of a Photographically Identified Population of Manta Rays (*Manta alfredi*) in Southern Mozambique. *Mar. Biol.* **2011**, *158*, 1111–1124. [[CrossRef](#)]
35. Couturier, L.I.E.; Dudgeon, C.L.; Pollock, K.H.; Jaine, F.R.A.; Bennett, M.B.; Townsend, K.A.; Weeks, S.J.; Richardson, A.J. Population Dynamics of the Reef Manta Ray (*Manta alfredi*) in Eastern Australia. *Coral Reefs* **2014**, *33*, 329–342. [[CrossRef](#)]
36. Braun, C.D.; Skomal, G.B.; Thorrold, S.R.; Berumen, M.L. Movements of the Reef Manta Ray (*Manta alfredi*) in the Red Sea Using Satellite and Acoustic Telemetry. *Mar. Biol.* **2015**, *162*, 2351–2362. [[CrossRef](#)]
37. Stewart, J.D.; Beale, C.S.; Fernando, D.; Sianipar, A.B.; Burton, R.S.; Semmens, B.X.; Aburto-Oropeza, O. Spatial Ecology and Conservation of *Manta birostris* in the Indo-Pacific. *Biol. Conserv.* **2016**, *200*, 178–183. [[CrossRef](#)]
38. Setyawan, E.; Sianipar, A.B.; Erdmann, M.V.; Fischer, A.M.; Haddy, J.A.; Beale, C.S.; Lewis, S.; Mambrasar, R. Site Fidelity and Movement Patterns of Reef Manta Rays (*Mobula alfredi*: Mobulidae) Using Passive Acoustic Telemetry in Northern Raja Ampat, Indonesia. *Nat. Conserv. Res.* **2018**, *3*, 1–15. [[CrossRef](#)]
39. Germanov, E.S.; Bejder, L.; Chabanne, D.B.H.; Dharmadi, D.; Hendrawan, I.G.; Marshall, A.D.; Pierce, S.J.; van Keulen, M.; Loneragan, N.R. Contrasting Habitat Use and Population Dynamics of Reef Manta Rays within the Nusa Penida Marine Protected Area, Indonesia. *Front. Mar. Sci.* **2019**, *6*, 215. [[CrossRef](#)]
40. Peel, L.R.; Stevens, G.M.W.; Daly, R.; Keating Daly, C.A.; Lea, J.S.E.; Clarke, C.R.; Collin, S.P.; Meekan, M.G. Movement and Residency Patterns of Reef Manta Rays (*Mobula alfredi*) in the Amirante Islands, Seychelles. *Mar. Ecol. Prog. Ser.* **2019**, *621*, 169–184. [[CrossRef](#)]
41. Andrzejczek, S.; Chapple, T.K.; Curnick, D.J.; Carlisle, A.B.; Castleton, M.; Jacoby, D.M.P.; Peel, L.R.; Schallert, R.J.; Tickler, D.M.; Block, B.A. Individual Variation in Residency and Regional Movements of Reef Manta Rays (*Mobula alfredi*) in a Large Marine Protected Area. *Mar. Ecol. Prog. Ser.* **2020**, *639*, 137–153.
42. Pate, J.H.; Marshall, A.D. Urban Manta Rays: Potential Manta Ray Nursery Habitat along a Highly Developed Florida Coastline. *Endanger. Species Res.* **2020**, *43*, 51–64.
43. Venables, S.K.; van Duinkerken, D.I.; Rohner, C.A.; Marshall, A.D. Habitat Use and Movement Patterns of Reef Manta Rays *Mobula alfredi* in Southern Mozambique. *Mar. Ecol. Prog. Ser.* **2020**, *634*, 99–114. [[CrossRef](#)]
44. Marshall, A.; Barreto, R.; Carlson, J.; Fernando, D.; Fordham, S.; Francis, M.P.; Herman, K.; Jabado, R.W.; Liu, K.M.; Pacoureaux, N.; et al. *Mobula alfredi*; The IUCN Red List of Threatened Species, 2019: E.T195459A68632178. Available online: <https://dx.doi.org/10.2305/IUCN.UK.2019-3.RLTS.T195459A68632178.en> (accessed on 24 February 2022).
45. Marshall, A.; Barreto, R.; Carlson, J.; Fernando, D.; Fordham, S.; Francis, M.P.; Derrick, D.; Herman, K.; Jabado, R.W.; Liu, K.M.; et al. *Mobula birostris*; The IUCN Red List of Threatened Species, 2020: E.T198921A68632946. Available online: <https://dx.doi.org/10.2305/IUCN.UK.2020-3.RLTS.T198921A68632946.en> (accessed on 24 February 2022).
46. Dulvy, N.K.; Fowler, S.L.; Musick, J.A.; Cavanagh, R.D.; Kyne, P.M.; Harrison, L.R.; Carlson, J.K.; Davidson, L.N.; Fordham, S.V.; Francis, M.P.; et al. Extinction Risk and Conservation of the World’s Sharks and Rays. *Elife* **2014**, *3*, e00590. [[CrossRef](#)]
47. Croll, D.A.; Dewar, H.; Dulvy, N.K.; Fernando, D.; Francis, M.P.; Galván-Magaña, F.; Hall, M.; Heinrichs, S.; Marshall, A.; Mccauley, D.; et al. Vulnerabilities and Fisheries Impacts: The Uncertain Future of Manta and Devil Rays. *Aquat. Conserv.* **2016**, *26*, 562–575. [[CrossRef](#)]
48. Lawson, J.M.; Fordham, S.V.; O’Malley, M.P.; Davidson, L.N.K.; Walls, R.H.L.; Heupel, M.R.; Stevens, G.; Fernando, D.; Budziak, A.; Simpfendorfer, C.A.; et al. Sympathy for the Devil: A Conservation Strategy for Devil and Manta Rays. *PeerJ* **2017**, *5*, e3027. [[CrossRef](#)]
49. Couturier, L.I.E.; Marshall, A.D.; Jaine, F.R.A.; Kashiwagi, T.; Pierce, S.J.; Townsend, K.A.; Weeks, S.J.; Bennett, M.B.; Richardson, A.J. Biology, Ecology and Conservation of the Mobulidae. *J. Fish Biol.* **2012**, *80*, 1075–1119. [[CrossRef](#)]
50. Stewart, J.D.; Jaine, F.R.A.; Armstrong, A.J.; Armstrong, A.O.; Bennett, M.B.; Burgess, K.B.; Couturier, L.I.E.; Croll, D.A.; Cronin, M.R.; Deakos, M.H.; et al. Research Priorities to Support Effective Manta and Devil Ray Conservation. *Front. Mar. Sci.* **2018**, *5*, 314. [[CrossRef](#)]
51. Perryman, R.J.Y. Social Organisation, Social Behaviour and Collective Movements in Reef Manta Rays. Ph.D. Thesis, Macquarie University, Sydney, Australia, 2020.
52. Setyawan, E.; Erdmann, M.V.; Lewis, S.A.; Mambrasar, R.; Hasan, A.W.; Templeton, S.; Beale, C.S.; Sianipar, A.B.; Shidqi, R.; Heuschkel, H.; et al. Natural History of Manta Rays in the Bird’s Head Seascape, Indonesia, with an Analysis of the Demography and Spatial Ecology of *Mobula alfredi* (Elasmobranchii: Mobulidae). *J. Ocean Sci. Found.* **2020**, *36*, 49–83.
53. Setyawan, E.; Stevenson, B.C.; Izuan, M.; Constantine, R.; Erdmann, M.V. How Big Is That Manta Ray? A Novel and Non-Invasive Method for Measuring Reef Manta Rays Using Small Drones. *Drones* **2022**, *6*, 63. [[CrossRef](#)]

54. Graham, R.T.; Witt, M.J.; Castellanos, D.W.; Remolina, F.; Maxwell, S.; Godley, B.J.; Hawkes, L.A. Satellite Tracking of Manta Rays Highlights Challenges to Their Conservation. *PLoS ONE* **2012**, *7*, e36834.
55. Armstrong, A.O.; Armstrong, A.J.; Jaine, F.R.A.; Couturier, L.I.E.; Fiora, K.; Uribe-Palomino, J.; Weeks, S.J.; Townsend, K.A.; Bennett, M.B.; Richardson, A.J. Prey Density Threshold and Tidal Influence on Reef Manta Ray Foraging at an Aggregation Site on the Great Barrier Reef. *PLoS ONE* **2016**, *11*, e0153393. [[CrossRef](#)]
56. Armstrong, A.O.; Stevens, G.M.W.; Townsend, K.A.; Murray, A.; Bennett, M.B.; Armstrong, A.J.; Uribe-Palomino, J.; Hosegood, P.; Dudgeon, C.L.; Richardson, A.J. Reef Manta Rays Forage on Tidally Driven, High Density Zooplankton Patches in Hanifaru Bay, Maldives. *PeerJ* **2021**, *9*, e11992. [[CrossRef](#)]
57. Fish, F.E.; Kolpas, A.; Crosssett, A.; Dudas, M.A.; Moored, K.W.; Bart-Smith, H. Kinematics of Swimming of the Manta Ray: Three-Dimensional Analysis of Open-Water Maneuverability. *J. Exp. Biol.* **2018**, *221*, jeb166041. [[CrossRef](#)]
58. Hinojosa-Alvarez, S.; Walter, R.P.; Diaz-Jaimes, P.; Galván-Magaña, F.; Paig-Tran, E.M. A Potential Third Manta Ray Species near the Yucatán Peninsula? Evidence for a Recently Diverged and Novel Genetic Manta Group from the Gulf of Mexico. *PeerJ* **2016**, *4*, e2586. [[CrossRef](#)]
59. Hosegood, J.; Humble, E.; Ogden, R.; de Bruyn, M.; Creer, S.; Stevens, G.M.W.; Abudaya, M.; Bassos-Hull, K.; Bonfil, R.; Fernando, D.; et al. Phylogenomics and Species Delimitation for Effective Conservation of Manta and Devil Rays. *Mol. Ecol.* **2020**, *29*, 4783–4796. [[CrossRef](#)]
60. Marshall, A.D.; Pierce, S.J. The Use and Abuse of Photographic Identification in Sharks and Rays. *J. Fish Biol.* **2012**, *80*, 1361–1379. [[CrossRef](#)]
61. Deakos, M.H. Paired-Laser Photogrammetry as a Simple and Accurate System for Measuring the Body Size of Free-Ranging Manta Rays (*Manta alfredi*). *Aquat. Biol.* **2010**, *10*, 1–10. [[CrossRef](#)]
62. Kinovea. Available online: <http://www.kinovea.org> (accessed on 1 July 2021).
63. Vogel, S. *Comparative Biomechanics: Life's Physical World-Second Edition*; Princeton University Press: Princeton, NJ, USA, 2013; ISBN 9780691155661.
64. Jodice, P.G.R.; Roby, D.D.; Suryan, R.M.; Irons, D.B.; Kaufman, A.M.; Turco, K.R.; Visser, G.H. Variation in Energy Expenditure among Black-Legged Kittiwakes: Effects of Activity-Specific Metabolic Rates and Activity Budgets. *Physiol. Biochem. Zool.* **2003**, *76*, 375–388. [[CrossRef](#)]
65. Paig-Tran, E.W.M.; Bizzarro, J.J.; Strother, J.A.; Summers, A.P. Bottles as Models: Predicting the Effects of Varying Swimming Speed and Morphology on Size Selectivity and Filtering Efficiency in Fishes. *J. Exp. Biol.* **2011**, *214*, 1643–1654. [[CrossRef](#)]
66. Hoffmann, S.L.; Porter, M.E. Body and Pectoral Fin Kinematics During Routine Yaw Turning in Bonnethead Sharks (*Sphyrna tiburo*). *Integr. Comp. Biol.* **2019**, *1*, 1–15.
67. Papastamatiou, Y.P.; DeSalles, P.A.; McCauley, D.J. Area-Restricted Searching by Manta Rays and Their Response to Spatial Scale in Lagoon Habitats. *Mar. Ecol. Prog. Ser.* **2012**, *456*, 233–244. [[CrossRef](#)]
68. Germanov, E.S.; Pierce, S.J.; Marshall, A.D.; Hendrawan, G.; Kefi, A.; Bejder, L.; Loneragan, N.R. Residency, movement patterns, behavior and demographics of reef manta rays in Komodo National Park. *PeerJ* **2022**, submitted.
69. Papastamatiou, Y.P.; Iosilevskii, G.; Di Santo, V.; Huvneers, C.; Hattab, T.; Planes, S.; Ballesta, L.; Mourier, J. Sharks Surf the Slope: Current Updrafts Reduce Energy Expenditure for Aggregating Marine Predators. *J. Anim. Ecol.* **2021**, *90*, 10. [[CrossRef](#)]
70. Pate, J.H.; (Marine Megafauna Foundation, West Palm Beach, FL, USA). Unpublished work on Nortek ECO ADCP deployment. 2020.
71. Venables, S. Short-Term Behavioural Responses of Manta Rays, *Manta alfredi*, to Tourism Interactions in Coral Bay, Western Australia. Bachelor's Thesis, Murdoch University, Murdoch, Australia, 2013.
72. Venables, S.; McGregor, F.; Brain, L.; van Keulen, M. Manta Ray Tourism Management, Precautionary Strategies for a Growing Industry: A Case Study from the Ningaloo Marine Park, Western Australia. *Pac. Conserv. Biol.* **2016**, *22*, 295–300. [[CrossRef](#)]
73. Noren, S.R.; Biedenbach, G.; Edwards, E.F. Ontogeny of Swim Performance and Mechanics in Bottlenose Dolphins (*Tursiops truncatus*). *J. Exp. Biol.* **2006**, *209*, 4724–4731. [[CrossRef](#)] [[PubMed](#)]
74. Marshall, A.D.; Bennett, M.B. Reproductive Ecology of the Reef Manta Ray *Manta alfredi* in Southern Mozambique. *J. Fish Biol.* **2010**, *77*, 169–190. [[CrossRef](#)] [[PubMed](#)]
75. Stevens, G.M.W.; Hawkins, J.P.; Roberts, C.M. Courtship and Mating Behaviour of Manta Rays *Mobula alfredi* and *M. birostris* in the Maldives. *J. Fish Biol.* **2018**, *93*, 344–359. [[CrossRef](#)]
76. Leos-Barajas, V.; Photopoulou, T.; Langrock, R.; Patterson, T.A.; Watanabe, Y.Y.; Murgatroyd, M.; Papastamatiou, Y.P. Analysis of Animal Accelerometer Data Using Hidden Markov Models. *Methods Ecol. Evol.* **2017**, *8*, 161–173. [[CrossRef](#)]
77. Whoriskey, K.; Auger-Méthé, M.; Albertsen, C.M.; Whoriskey, F.G.; Binder, T.R.; Krueger, C.C.; Mills Flemming, J. A Hidden Markov Movement Model for Rapidly Identifying Behavioral States from Animal Tracks. *Ecol. Evol.* **2017**, *7*, 2112–2121. [[CrossRef](#)]
78. Brewster, L.R.; Dale, J.J.; Guttridge, T.L.; Gruber, S.H.; Hansell, A.C.; Elliott, M.; Cowx, I.G.; Whitney, N.M.; Gleiss, A.C. Development and Application of a Machine Learning Algorithm for Classification of Elasmobranch Behaviour from Accelerometry Data. *Mar. Biol.* **2018**, *165*, 62. [[CrossRef](#)]
79. Divi, R.V.; Strother, J.A.; Paig-Tran, E.W.M. Manta Rays Feed Using Ricochet Separation, a Novel Nonclogging Filtration Mechanism. *Sci. Adv.* **2018**, *4*, eaat9533. [[CrossRef](#)]
80. Lawson, C.L.; Halsey, L.G.; Hays, G.C.; Dudgeon, C.L.; Payne, N.L.; Bennett, M.B.; White, C.R.; Richardson, A.J. Powering Ocean Giants: The Energetics of Shark and Ray Megafauna. *Trends Ecol. Evol.* **2019**, *34*, 1009–1021. [[CrossRef](#)]